10th ANKARA INTERNATIONAL AEROSPACE CONFERENCE **AIAC-2019-161**
18-20 September 2019 - METU, Ankara TURKEY

A THERMAL EQUILIBRIUM ANALYSIS FROM PARTICLE ACTIVITY PERSPECTIVE USING MOLECULAR DYNAMICS SIMULATION

İsmail Kabakcı[1], Cahit Çıray[2] and Demirkan Çöker[3]
Middle East Technical University
Ankara, Turkey

ABSTRACT

One important objective of engineering is to provide simplified models describing the behavior of the matter in nature. No doubt the use of continuum approach helps in this way and enables to make quantitative estimations for many problems from the engineering point of view. However, there are still some problems, such as turbulence and phenomena leading to turbulence, very far from a thorough understanding and of generalized tools of estimation. Molecular dynamics simulation techniques are popular to investigate problems in particle activity basis; hence they are utilized in a simulation code set, developed in MATLAB, and applied to thermal diffusion problem in the scope of this work. Two separate and isolated systems of Argon particles at different mean temperatures are defined and establishment of the equilibrium state is examined. Afterwards, the separation is removed and particles of two systems are allowed to interact. Behavior of the particles is modeled as simple particles in this study. Therefore, only translational motion of particles is considered, neglecting rotational motion. Simulation results imply the diffusion of the thermal energy between two systems and establishment of the new equilibrium state in the new system of particles is observed from different aspects.

INTRODUCTION

There was a suggestion of investigating turbulence and phenomena leading to turbulence from the particle activity perspective with a provided formulation for this purpose [Çıray, 2015]. Validation of this approach for an isolated system of particles in static conditions was performed previously as a Master's Thesis [Eneren, 2016]. A similar formulation is derived in order to calculate the velocities and positions of particles after interactions. Different to available study, effects of instantaneous velocities and interactions are calculated separately during the derivation of the formulation. In the scope of this work, an initial set up consisting of two separated and well insulated systems of 1000 Argon particles each at two different temperatures is considered as visualized in Figure 1. Establishment of the equilibrium state is satisfied in both systems first. Thermal diffusion, taking place between particles of each system, is simulated after the removal of the separation. A simulation code set is developed in MATLAB for this purpose. The method, followed in the approach, is compared to the available data in literature. At the equilibrium state; simulation results, the probability density function of

---

[1] MSc. Student in Aerospace Engineering Department, Email: ikabakci@ae.metu.edu.tr
[2] Prof. Emer. Dr. in Aerospace Engineering Department, Email: cciray@metu.edu.tr
[3] Assoc. Prof. Dr. in Aerospace Engineering Department, Email: coker@metu.edu.tr

the speed distribution and the velocity distribution along coordinate axes are compared with the theoretical values, the Maxwell-Boltzmann and Gaussian distributions respectively. Also, the fluid pressures acting at boundaries and mid-planes are checked in compliance with the literature. In the scope of diffusion dynamics analyses; establishment of equilibrium state is examined, particle and volume based thermal equilibrium analyses are performed and thermal conductivity coefficient is calculated.

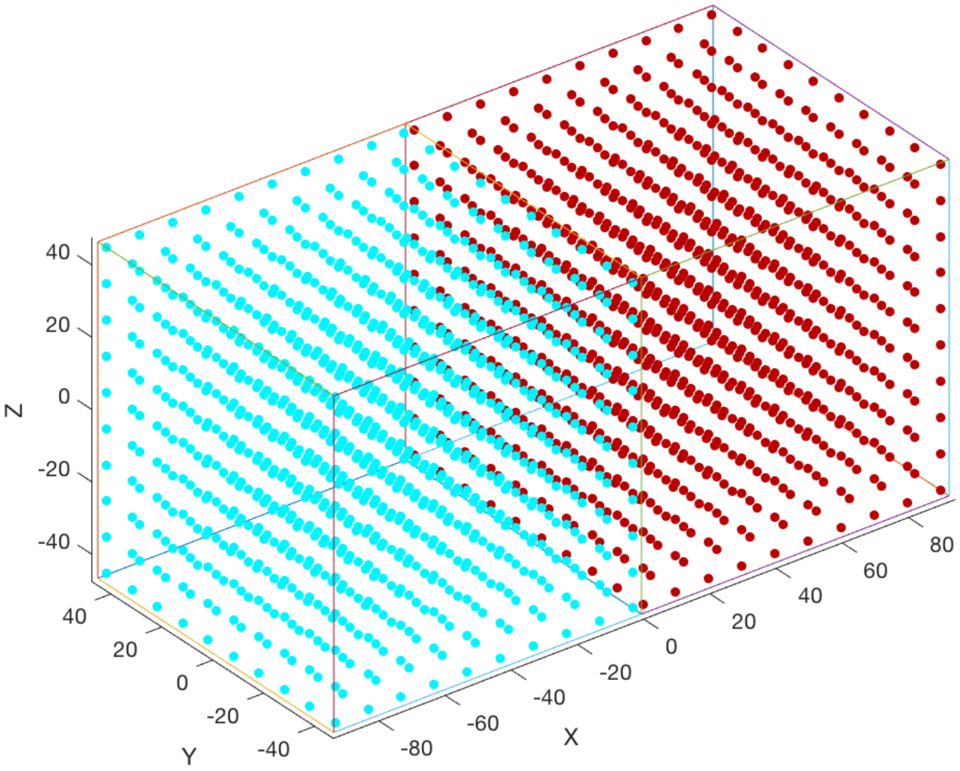

Figure 1: The Initial Set Up of the Problem

Motivation of the Study

Although this work does not contain any flow activity and the application is not a turbulence problem, it is expected to imply the feasibility of the approach and inspire for further studies about turbulent flow from the same point of view. The number of particles and duration of the simulation shall increase for these studies. Since errors will accumulate in larger systems and longer durations, the accuracy of the method will be critical. This study aims to increase the accuracy by taking the motion of particles into consideration. In the latest related study [Eneren, 2016]; particles were frozen at the initial state of iterations and all potential arising from the distance between particles was converted to kinetic energy. Since the potentials are large when a particle enters a fictitious shell of another, Eneren overcame this case by moving the particle to the equilibrium distance. The approach in this study is to estimate the next potential of any interacting particle in order to enhance velocity distribution accuracy. Due to the use of small time step in molecular dynamics simulations, the motion of particles is highly restricted. Therefore, effects of previous state and interaction are calculated separately.

METHOD

Base Formulation

The method is introduced to formulate the motion of particles using Newton's 2nd Law of Motion and Force Potential Theory.

A simple particle (e.g. particle i) of mass m_i is subjected to a force $\boldsymbol{F}_{ij}^{*}$ as a result of the interaction with any of the surrounding simple particles (e.g. particle j). Positions of particle i and particle j are denoted by $\boldsymbol{r}_i$ and $\boldsymbol{r}_j$ respectively. Total force acting on particle i ($\boldsymbol{F}_i$) is the sum of pair interactions of surrounding j particles:

$$\boldsymbol{F}_i = \sum_{\substack{j=1 \\ (j \neq i)}}^{N} \boldsymbol{F}_{ij}^{*} \tag{1}$$

where * symbol is used to denote the interaction between only two particles (the pair interaction) is taken into consideration. Note that these pair forces are the same in magnitude but opposite in direction. Direction of the force acting on particle i is selected as the positive direction of the pair force for convention. A consequence of the Newton's 2nd Law of Motion:

$$\frac{d\boldsymbol{U}_i}{dt} = \sum_{\substack{j=1 \\ (j \neq i)}}^{N} \frac{d\boldsymbol{U}_i^{*}(j, \Delta t)}{dt} \tag{2}$$

where t is time, and $\boldsymbol{U}_i$ is the velocity vector of the particle i. Equation 2 shows that the velocity of a particle can be calculated easily if velocity contributions of pair interactions can be determined. Integrating Equation 2 with respect to time between the starting and ending phases of the one simulation step, namely a simulation time step (Δt):

$$\boldsymbol{U}_i(t + \Delta t) - \boldsymbol{U}_i(t) = \sum_{\substack{j=1 \\ (j \neq i)}}^{N} \left[\boldsymbol{U}_i^{*}(j, t + \Delta t) - \boldsymbol{U}_i^{*}(j, t)\right] \tag{3}$$

$$\boldsymbol{U}_i(t + \Delta t) = \boldsymbol{U}_i(t) + \sum_{\substack{j=1 \\ (j \neq i)}}^{N} \boldsymbol{\Delta U}_i^{*}(j, \Delta t) \tag{4}$$

where $\boldsymbol{\Delta U}_i^{*}(j, \Delta t)$ is the velocity contribution of any surrounding j particle on particle i during simulation time step. Equation 4 enables to find resulting velocities of particles in the system at the end of a selected simulation time step in the form of velocity contribution summations.

Pair interaction force between two neighbor particles can be modified in the following form:

$$\boldsymbol{F}_{ij}^{*}\left(r_{ij}^{*}\right) = m_i \frac{d\boldsymbol{U}_i^{*}}{dr_{ij}^{*}} \frac{dr_{ij}^{*}}{dt} \tag{5}$$

where $\boldsymbol{r}_{ij}$ is the relative position vector of particle i with respect to particle j and r_{ij} is the absolute scalar form of $\boldsymbol{r}_{ij}$. Applying the Chain Rule for differentiation in Equation 5:

$$\boldsymbol{F}_{ij}^{*}\left(r_{ij}^{*}\right) = m_i \frac{d\boldsymbol{U}_i^{*}}{dr_{ij}^{*}} \left[\frac{dr_{ij}^{*}}{dx_{ij}^{*}} \frac{dx_{ij}^{*}}{dt} + \frac{dr_{ij}^{*}}{dy_{ij}^{*}} \frac{dy_{ij}^{*}}{dt} + \frac{dr_{ij}^{*}}{dz_{ij}^{*}} \frac{dz_{ij}^{*}}{dt}\right] \tag{6}$$

The distance between the particles is simply the square-root of the sum of the squares of distances along the coordinate axes. Calculating the derivatives accordingly and writing in a vector form:

7
$$\boldsymbol{F}^*_{\boldsymbol{ij}}\left(r^*_{ij}\right) = m_i \frac{\boldsymbol{r}^*_{\boldsymbol{ij}}\left(\boldsymbol{U}^*_{\boldsymbol{i}} - \boldsymbol{U}^*_{\boldsymbol{j}}\right)}{r^*_{ij}} \frac{d\boldsymbol{U}^*_{\boldsymbol{i}}}{dr^*_{ij}}$$

Since pair interaction forces are the same in magnitude but opposite in direction, Equation 9 is valid:

8
$$\frac{d\boldsymbol{U}^*_{\boldsymbol{i}}}{dr^*_{ij}} \frac{dr^*_{ij}}{dt} = -\frac{m_j}{m_i} \frac{d\boldsymbol{U}^*_{\boldsymbol{j}}}{dr^*_{ij}} \frac{dr^*_{ij}}{dt}$$

9
$$\frac{d\boldsymbol{U}^*_{\boldsymbol{i}}}{dr^*_{ij}} = -\frac{m_j}{m_i} \frac{d\boldsymbol{U}^*_{\boldsymbol{j}}}{dr^*_{ij}}$$

This enables to rewrite Equation 7 as:

10
$$\boldsymbol{F}^*_{\boldsymbol{ij}}\left(r^*_{ij}\right) = m_i \frac{\boldsymbol{r}^*_{\boldsymbol{ij}}}{r^*_{ij}} \left[\frac{d}{dr^*_{ij}}\left(\frac{U_i^{*2}}{2}\right) + \frac{m_j}{m_i} \frac{d}{dr^*_{ij}}\left(\frac{U_j^{*2}}{2}\right)\right]$$

Note that pair force is in the direction of the line connecting center of the particles in Equation 10 as expected. Considering the force potential theory, the mutual force on particle i under the effect of particle j is described by the following equation:

11
$$\boldsymbol{F}^*_{\boldsymbol{ij}}\left(r^*_{ij}\right) = -\,\boldsymbol{\nabla}_{\boldsymbol{r}^*_i}\, \psi_{ij}\left(r^*_{ij}\right)$$

12
$$\boldsymbol{F}^*_{\boldsymbol{ij}}\left(r^*_{ij}\right) = -\left(\frac{\partial r^*_{ij}}{\partial x^*_i}\boldsymbol{e_x} + \frac{\partial r^*_{ij}}{\partial y^*_i}\boldsymbol{e_y} + \frac{\partial r^*_{ij}}{\partial z^*_i}\boldsymbol{e_z}\right) \frac{d\psi_{ij}\left(r^*_{ij}\right)}{dr^*_{ij}}$$

13
$$\boldsymbol{F}^*_{\boldsymbol{ij}}\left(r^*_{ij}\right) = -\left(\frac{x^*_{ij}}{r^*_{ij}}\boldsymbol{e_x} + \frac{y^*_{ij}}{r^*_{ij}}\boldsymbol{e_y} + \frac{z^*_{ij}}{r^*_{ij}}\boldsymbol{e_z}\right) \frac{d\psi_{ij}\left(r^*_{ij}\right)}{dr^*_{ij}}$$

14
$$\boldsymbol{F}^*_{\boldsymbol{ij}}\left(r^*_{ij}\right) = -\frac{\boldsymbol{r}^*_{\boldsymbol{ij}}}{r^*_{ij}} \frac{d\psi^*_{ij}}{dr^*_{ij}}$$

where ψ_{ij} term represents the so-called force potential between i and j particles. Note that Equation 10 and Equation 14 describe the same pair force from two different perspectives and they are equal. Therefore, these two equations can be combined as:

15
$$m_i \frac{\boldsymbol{r}^*_{\boldsymbol{ij}}}{r^*_{ij}} \left[\frac{d}{dr^*_{ij}}\left(\frac{U_i^{*2}}{2}\right) + \frac{m_j}{m_i} \frac{d}{dr^*_{ij}}\left(\frac{U_j^{*2}}{2}\right)\right] + \frac{\boldsymbol{r}^*_{\boldsymbol{ij}}}{r^*_{ij}} \frac{d\psi^*_{ij}}{dr^*_{ij}} = 0$$

16
$$\frac{1}{2}\left[m_i \frac{dU_i^{*2}}{dr^*_{ij}} + m_j \frac{dU_j^{*2}}{dr^*_{ij}}\right] + \frac{d\psi^*_{ij}}{dr^*_{ij}} = 0$$

which shows that sum of kinetic and potential energy terms is constant during interaction. Rearranging and integrating Equation 16 between two simulation time steps:

$$\left[U_i^{*2}(t+\Delta t) - U_i^{*2}(t) + \frac{m_j}{m_i}\left[U_j^{*2}(t+\Delta t) - U_j^{*2}(t)\right]\right] + \frac{2}{m_i}\left[\psi_{ij}^{*}(t+\Delta t) - \psi_{ij}^{*}(t)\right] = 0 \tag{17}$$

$$\psi_{ij}^{*}(t+\Delta t) - \psi_{ij}^{*}(t) = \Phi_{ij}^{*}(\Delta t) \tag{18}$$

The term given in Equation 18, which also appears in Equation 17, represents the potential change during the time step. Between any two particles, separated by a distance, there exist a potential energy which appears molecular dynamics simulation formulations. Physicists developed several approaches to represent this potential. In his study, Lennard-Jones presented a model describing the repulsive and attractive parts of molecular field, the first form of the so-called Lennard-Jones Potential, in order to explain the equation state of a gas using available experimental data [Jones, 1924]. In this method, Lennard-Jones potential model, given in Equation 19, is utilized.

$$\psi_{ij}(r_{ij}) = 4\varepsilon\left[\left(\frac{\sigma}{r_{ij}}\right)^{12} - \left(\frac{\sigma}{r_{ij}}\right)^{6}\right] \tag{19}$$

where ε is the well-depth which is a measure of attraction strength and σ is the equilibrium distance (also referred to as van der Waals radius) defined as the distance where the intermolecular potential between the particles is zero.

For velocity of particles and their contributions, following relations can be used in Equation 17:

$$\boldsymbol{U_i^*}(t+\Delta t) = \boldsymbol{U_i^*}(t) + \boldsymbol{\Delta U_i^*}(j,\Delta t) \tag{20}$$

$$\boldsymbol{\Delta U_i^*}(j,\Delta t) = \Delta U_{x,i}^{*}(j,\Delta t)\boldsymbol{e_x} + \Delta U_{y,i}^{*}(j,\Delta t)\boldsymbol{e_y} + \Delta U_{z,i}^{*}(j,\Delta t)\boldsymbol{e_z} \tag{21}$$

$$U_i^{*2}(t+\Delta t) = U_{x,i}^{*2}(t+\Delta t) + U_{y,i}^{*2}(t+\Delta t) + U_{z,i}^{*2}(t+\Delta t) \tag{22}$$

$$U_{x,i}^{*2}(t+\Delta t) = U_{x,i}^{*2}(t) + 2U_{x,i}^{*}(t)\Delta U_{x,i}^{*}(j,\Delta t) + \Delta U_{x,i}^{*2}(j,\Delta t) \tag{23}$$

Note that, four equations above are also applicable for surrounding j particles. Furthermore, Equation 23 can be expressed in y and z directions similarly. Due to conservation of momentum, Equation 24 is valid:

$$\boldsymbol{\Delta U_j^*}(i,\Delta t) = -\frac{m_i}{m_j}\boldsymbol{\Delta U_i^*}(j,\Delta t) \tag{24}$$

where $\boldsymbol{\Delta U_i^*}(j,\Delta t)$ term is used to describe the velocity contribution for particle i due to the interaction with particle j during Δt time step. Applying Equations 19-24, Equation 18 takes the following form:

$$\begin{aligned} &\Delta U_i^{*2}(j,\Delta t) + 2\boldsymbol{U_i^*}(t)\boldsymbol{\Delta U_i^*}(j,\Delta t) \\ &\quad + \frac{m_j}{m_i}\left[\left(\frac{m_i}{m_j}\right)^{2}\Delta U_i^{*2}(j,\Delta t) - 2\left(\frac{m_i}{m_j}\right)\boldsymbol{U_j^*}(t)\boldsymbol{\Delta U_i^*}(j,\Delta t)\right] + \frac{2}{m_i}\Phi_{ij}^{*}(\Delta t) \\ &\quad = 0 \end{aligned} \tag{25}$$

26

$$\left(1+\frac{m_i}{m_j}\right)\Delta U_i^{*2}(j,\Delta t)+2\left[\boldsymbol{U_i^*}(t)-\boldsymbol{U_j^*}(t)\right]\boldsymbol{\Delta U_i^*}(j,\Delta t)+\frac{2}{m_i}\Phi_{ij}^*(\Delta t)=0$$

27

$$\begin{aligned}\left(1+\frac{m_i}{m_j}\right)&\left[\Delta U_{x,i}^{*}{}^2(j,\Delta t)+\Delta U_{y,i}^{*}{}^2(j,\Delta t)+\Delta U_{z,i}^{*}{}^2(j,\Delta t)\right]\\&+2\Big[\left(U_{x,i}^*(t)-U_{x,j}^*(t)\right)\Delta U_{x,i}^*(j,\Delta t)\\&+\left(U_{y,i}^*(t)-U_{y,j}^*(t)\right)\Delta U_{y,i}^*(j,\Delta t)+\left(U_{z,i}^*(t)-U_{z,j}^*(t)\right)\Delta U_{z,i}^*(j,\Delta t)\Big]\\&+\frac{2}{m_i}\Phi_{ij}^*(\Delta t)=0\end{aligned}$$

Estimation of the Next Potential

As described in Equation 18, the formulation needs an estimation of the next potential at the end of time step. Lennard-Jones potential is utilized for estimation of the next potential. Only the interaction between two particles should be taken into consideration for this change because the effect of the previous state and interaction is separately calculated.

28

$$m_i\frac{d^2\boldsymbol{r_i^*}}{dt^2}=-\frac{\boldsymbol{r_{ij}^*}}{r_{ij}^*}\frac{d\psi_{ij}^*}{dr_{ij}^*}$$

29

$$m_i\frac{d^2\boldsymbol{r_i^*}}{dt^2}=-\frac{\boldsymbol{r_{ij}^*}}{r_{ij}^*}\left\{-\frac{24\varepsilon}{r_{ij}^*}\left[2\left(\frac{\sigma}{r_{ij}^*}\right)^{12}-\left(\frac{\sigma}{r_{ij}^*}\right)^{6}\right]\right\}$$

30

$$\frac{d^2\boldsymbol{r_i^*}}{dt^2}=\frac{\boldsymbol{r_{ij}^*}}{r_{ij}^*}\left\{\frac{24\varepsilon}{m_i r_{ij}^*}\left[2\left(\frac{\sigma}{r_{ij}^*}\right)^{12}-\left(\frac{\sigma}{r_{ij}^*}\right)^{6}\right]\right\}$$

Since the motion of particles is restricted, accelerations do not change significantly during time step. By this assumption, next distance and next potential between interacting particles can be estimated.

31

$$\boldsymbol{r_{ij}^*}(t+\Delta t)=\boldsymbol{r_{ij}^*}(t)+\frac{1}{2}\frac{d^2\boldsymbol{r_{ij}^*}(j,\Delta t)}{dt^2}\,\Delta t^2$$

32

$$\boldsymbol{r_{ij}^*}(t+\Delta t)=\boldsymbol{r_{ij}^*}(t)+\left\{\left(\frac{m_i+m_j}{m_i\,m_j}\right)\frac{12\varepsilon}{r_{ij}^{*}{}^2(t)}\left[2\left(\frac{\sigma}{r_{ij}^*(t)}\right)^{12}-\left(\frac{\sigma}{r_{ij}^*(t)}\right)^{6}\right]\boldsymbol{r_{ij}^*(t)}\right\}\Delta t^2$$

33

$$\psi_{ij}(t+\Delta t)=4\varepsilon\left[\left(\frac{\sigma}{r_{ij}^*(t+\Delta t)}\right)^{12}-\left(\frac{\sigma}{r_{ij}^*(t+\Delta t)}\right)^{6}\right]$$

Relations of Velocity Contributions

Equation 27 is insufficient to describe the interaction itself because there are still unknown velocity contributions in each direction. As found in Equation 10 and being compatible with Newton's 2nd Law of Motion; the acceleration vector, arising due to the interaction, is along the line connecting particle centers. Therefore; the force and the velocity contribution should also be along the same line which implies the relation of velocity contributions in each direction, as Figure 2 describes an attraction case in two dimensions.

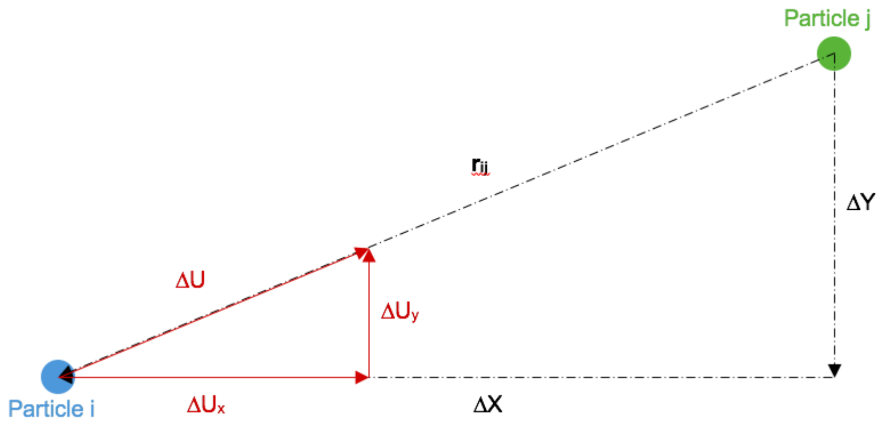

Figure 2: Attractive Velocity Contribution of One Particle on Another

Note that velocity contribution vector is a unit vector, just describing the direction. The velocity contribution is the multiplication of the average acceleration and simulation time step during interaction:

$$\boldsymbol{\Delta U}_i^*(j,\Delta t) = \frac{\overline{d^2 \boldsymbol{r}_i^*(j,\Delta t)}}{dt^2}\Delta t \qquad (34)$$

To determine average accelerations, the acceleration of particle i can be calculated using the distance between the particles for the start and finish set up:

$$\frac{\overline{d^2 r_{x,i}^*(j,\Delta t)}}{dt^2} = \frac{1}{2}\left[\frac{d^2 r_{x,i}^*(j,t+\Delta t)}{dt^2} + \frac{d^2 r_{x,i}^*(j,t)}{dt^2}\right] \qquad (35)$$

$$\frac{\Delta U_{x,i}^*(j,\Delta t)}{\Delta U_{y,i}^*(j,\Delta t)} = \frac{\dfrac{\overline{d^2 r_{x,i}^*(j,\Delta t)}}{dt^2}}{\dfrac{\overline{d^2 r_{y,i}^*(j,\Delta t)}}{dt^2}} = \frac{\dfrac{d^2 r_{x,i}^*(j,t+\Delta t)}{dt^2} + \dfrac{d^2 r_{x,i}^*(j,t)}{dt^2}}{\dfrac{d^2 r_{y,i}^*(j,t+\Delta t)}{dt^2} + \dfrac{d^2 r_{y,i}^*(j,t)}{dt^2}} \qquad (36)$$

$$\frac{\Delta U_{x,i}^*(j,\Delta t)}{\Delta U_{y,i}^*(j,\Delta t)} = \frac{\dfrac{\Delta X(t+\Delta t)}{r_{ij}(t+\Delta t)} + \dfrac{\Delta X(t)}{r_{ij}(t)}}{\dfrac{\Delta Y(t+\Delta t)}{r_{ij}(t+\Delta t)} + \dfrac{\Delta Y(t)}{r_{ij}(t)}} = \frac{\Delta X(t+\Delta t)\, r_{ij}(t) + \Delta X(t)\, r_{ij}(t+\Delta t)}{\Delta Y(t+\Delta t)\, r_{ij}(t) + \Delta Y(t)\, r_{ij}(t+\Delta t)} = \frac{k_x}{k_y} \qquad (37)$$

where k_x and k_y parameters are used to simplify the relations. Next positions are estimated using Equation 32. The remedy is also applicable in z-direction and following relation can be written:

$$k = \sqrt{\mathrm{k}_{\mathrm{x}}^2 + k_y^2 + k_z^2} \qquad (38)$$

Using these relations, Equation 27 can be reduced to one unknown:

$$\left(1+\frac{m_i}{m_j}\right)\left[\frac{k_x^2+k_y^2+k_z^2}{k_x^2}\right]\Delta U_{x,i}^{*}{}^{2}(j,\Delta t) + 2\left[\left(U_{x,i}^{*}(t)-U_{x,j}^{*}(t)\right)+\left(U_{y,i}^{*}(t)-U_{y,j}^{*}(t)\right)\frac{k_y}{k_x} + \left(U_{z,i}^{*}(t)-U_{z,j}^{*}(t)\right)\frac{k_z}{k_x}\right]\Delta U_{x,i}^{*}(j,\Delta t)+\frac{2}{m_i}\Phi_{ij}^{*}(\Delta t)=0 \tag{39}$$

$$\left(1+\frac{m_i}{m_j}\right)\frac{k^2}{k_x}\Delta U_{x,i}^{*}{}^{2}(j,\Delta t) + 2\left[\left(U_{x,i}^{*}(t)-U_{x,j}^{*}(t)\right)k_x+\left(U_{y,i}^{*}(t)-U_{y,j}^{*}(t)\right)k_y + \left(U_{z,i}^{*}(t)-U_{z,j}^{*}(t)\right)k_z\right]\Delta U_{x,i}^{*}(j,\Delta t)+\frac{2k_x}{m_i}\Phi_{ij}^{*}(\Delta t)=0 \tag{40}$$

Separation of Previous State and Interaction Effects

Since time step is kept very small during molecular dynamic simulations, the motion of the particles is highly restricted. Therefore, effect of previous velocities and interactions can be calculated separately which provides a significant simplification and time efficiency in simulation process. In other words, particles are assumed stationary at the start of the iteration and interactions take place with other particles during the small time step. Afterwards, present velocity of the particle is added in calculations. Therefore, the velocity contributions due to the interaction can be determined using Equation 41 and relations of velocity contributions as given in Equation 37. The γ term takes -1 or +1 value depending on the interaction being attractive or repulsive respectively.

$$\Delta U_{x,i}^{*}(j,\Delta t)=\gamma\frac{k_x}{k}\sqrt{\frac{-2m_j}{(m_i+m_j)m_i}\Phi_{ij}^{*}(\Delta t)} \tag{41}$$

Interaction between Unlike Molecules

When the interaction of two dissimilar non-bonded atoms takes place in simulations, the potential energy definitions are still used with the help of combining rules. Lorentz-Berthelot Combination Rule can be applied in Equation 41, taking its ease of implementation into consideration. The Rule suggests to use the arithmetic mean of the equilibrium distance and the geometric mean of the well-depth.

$$\sigma=\frac{\sigma_i+\sigma_j}{2} \tag{42}$$

$$\varepsilon=\sqrt{\varepsilon_i\varepsilon_j} \tag{43}$$

RESULTS

Along the positive side of X axis, 1000 Argon particles were placed at a temperature of 300 K. Also, 1000 Argon particles were placed at a temperature of 120 K along the negative side of X axis as shown in Figure 1. First phase of the simulation, where both systems were separated in order to reach their equilibrium state, took place about 50 picoseconds. Afterwards, the separation was removed and the second phase of the simulation took place about 100 picoseconds.

Establishment of the Equilibrium State

At the end of the first phase of the simulation, the visual interpretation of the state is given in Figure 3. Corresponding speeds of all particles are represented in “jet colormap array” of MATLAB. Color scheme of the array is provided in Figure 4. Dark blue color tones express low speeds while dark red color tones are used to represent high speeds.

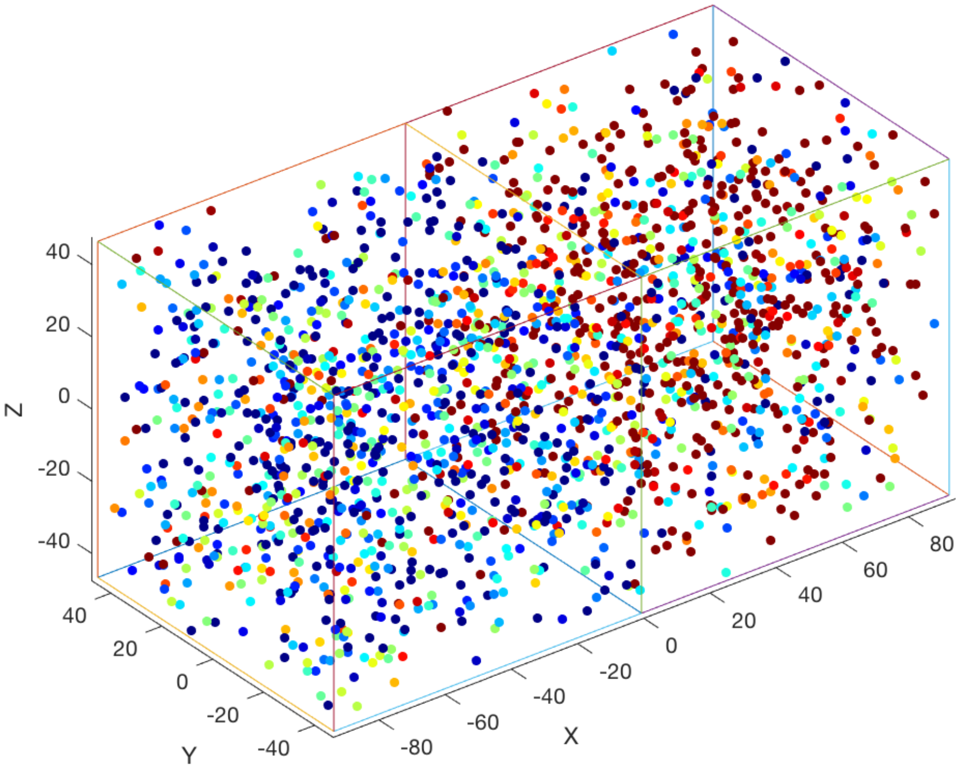

Figure 3: Visual Interpretation of the State at the End of the First Phase

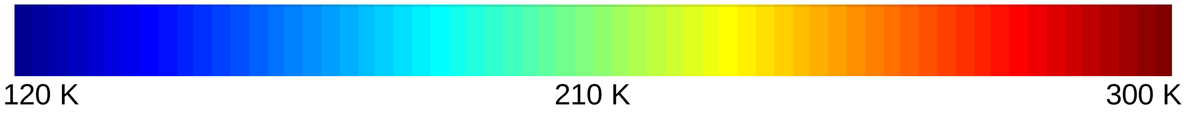

Figure 4: Jet Colormap Array

As it can be indicated from Figure 3, particles have various speeds in equilibrium condition. Speed distribution of ideal gases in equilibrium is described with the Maxwell-Boltzmann distribution. Also, velocity contributions along coordinate axes should comply with the Gaussian distribution at the equilibrium state. In Figure 5 and Figure 6, speed distributions and velocity contributions along the x-axis of both systems are compared with the Maxwell-Boltzmann and Gaussian distributions.

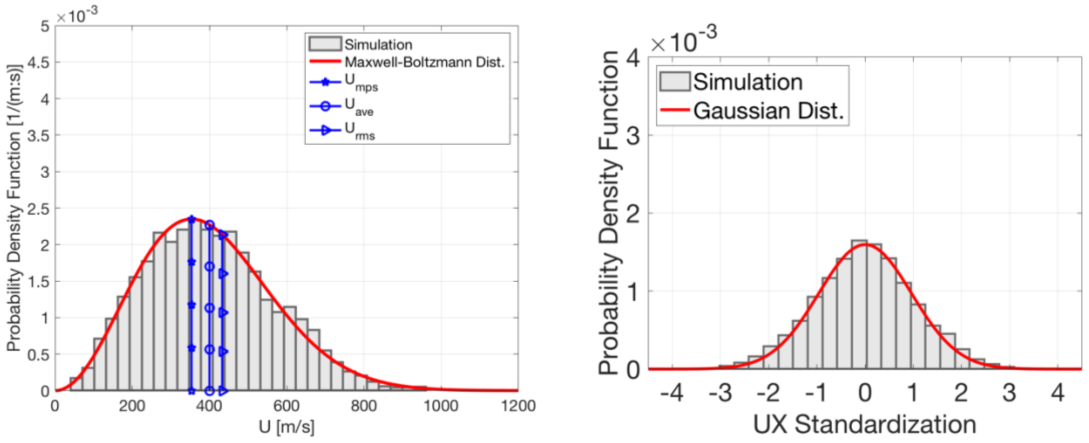

Figure 5: Speed Distribution and Velocity Contribution (x-axis) of the System at 300 K

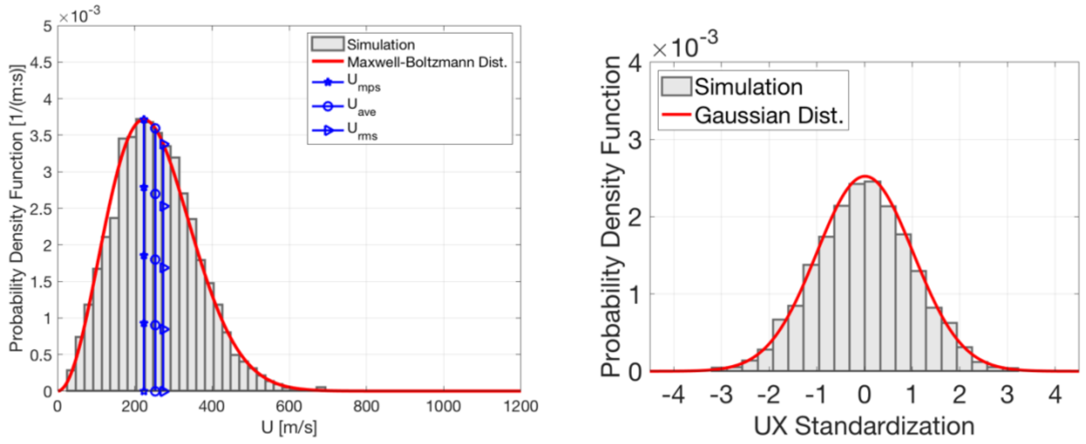

Figure 6: Speed Distribution and Velocity Contribution (x-axis) of the System at 120K

In Table 1, the most probable speed, average speed and root mean square (rms) speed obtained by this study are compared with the theoretical values and the results presented in Eneren's study [Eneren, 2016] in order to reveal the improvement in accuracy.

	Average Temperature [K]	**Most Probable Speed [m/s]**	**Average Speed [m/s]**	**rms Speed [m/s]**
Theoretical	120	223.5	252.2	273.8
Eneren's Simulation		228.1 *(+2.06%)*	250.2 *(-0.79%)*	273.9 *(+0.03%)*
Improved Simulation		223.5 *(0.00%)*	254.0 *(+0.71%)*	273.7 *(-0.03%)*
Theoretical	300	353.4	398.8	432.8
Eneren's Simulation		346.0 *(+2.10%)*	389.8 *(-2.26%)*	432.9 *(+0.03%)*
Improved Simulation		353.4 *(0.00%)*	398.8 *(0.00%)*	432.8 *(0.00%)*

Table 1: Comparison of Theoretical and Simulation Speeds

Gas pressure of two separated systems at boundaries and mid-planes, theoretical pressure obtained from the ideal gas pressure equation and their difference are presented in Table 2.

Average Temperature [K]	**Theoretical Pressure [kPa]**	**Simulation Pressure [kPa]**		**Difference [%]**	
		Boundaries	**Midplanes**	**Boundaries**	**Midplanes**
120	52.17	51.97	52.59	-0.38	0.81
300	130.44	130.37	130.43	-0.05	-0.01

Table 2: Gas Pressures at the End of the First Phase

The state and the speed distribution at the end of the second phase (mixing phase) are represented in Figure 7 and Figure 8 respectively.

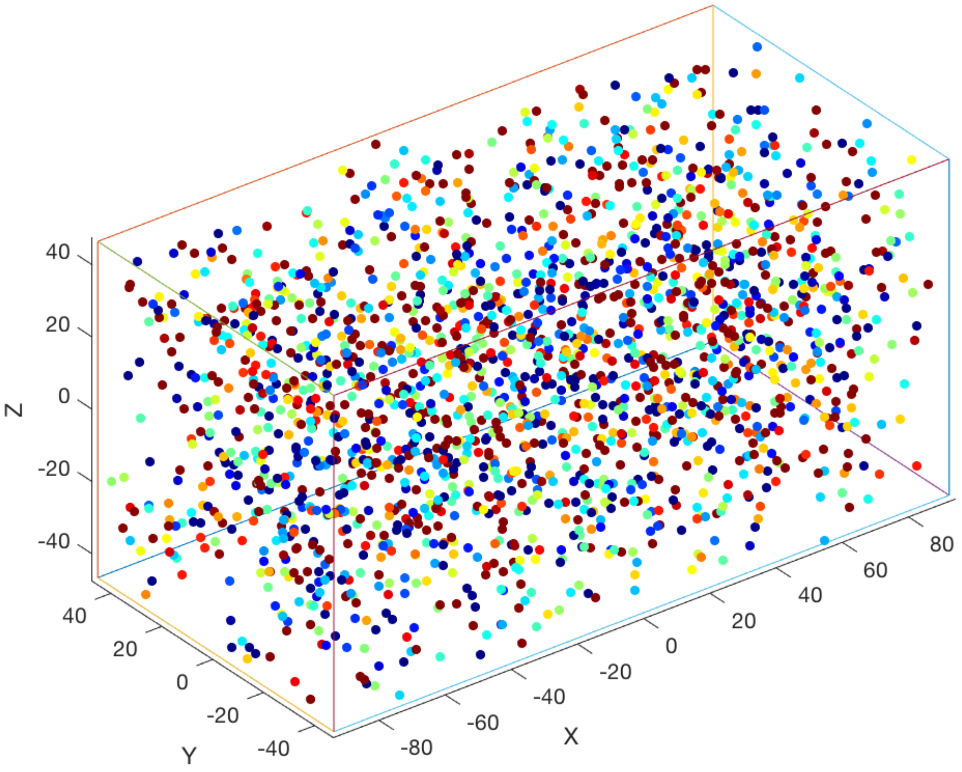

Figure 7: Visual Interpretation of the State at the End of the Second Phase

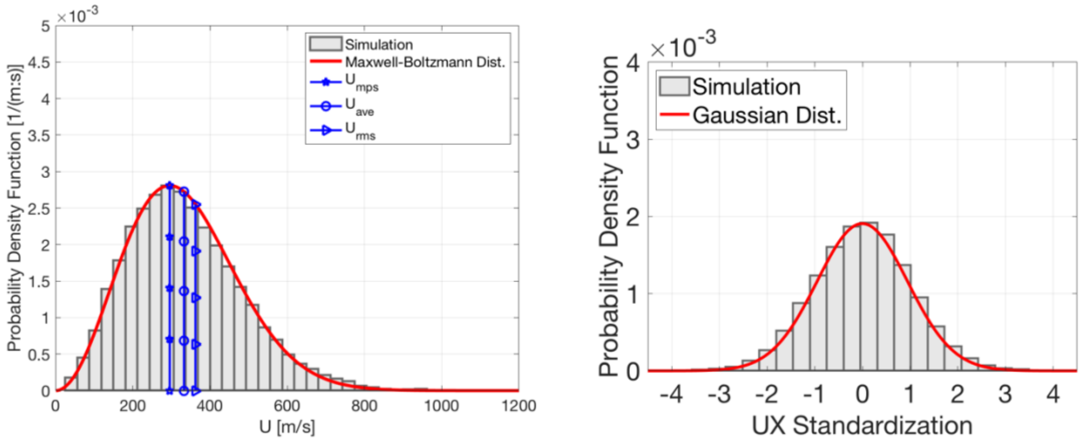

Figure 8: Speed Distribution and Velocity Contribution (x-axis) of the Final System

Gas pressure of the mixture at boundaries and mid-planes, expected theoretical pressures and their differences are presented in Table 3.

Average Temperature [K]	Theoretical Pressure [kPa]	Simulation Pressure [kPa]		Difference [%]	
		Boundaries	Midplanes	Boundaries	Midplanes
210	91.30	91.41	91.33	0.12	0.03

Table 3: Gas Pressures at the End of the Second Phase

Particle-Tracking Based Thermal Equilibrium Analysis: If particles are grouped as hot and cold system particles according to their initial states, visual interpretation of the state at the end of the second phase is provided in Figure 9 and average temperature of particles groups during phases of the simulation is shown in Figure 10.

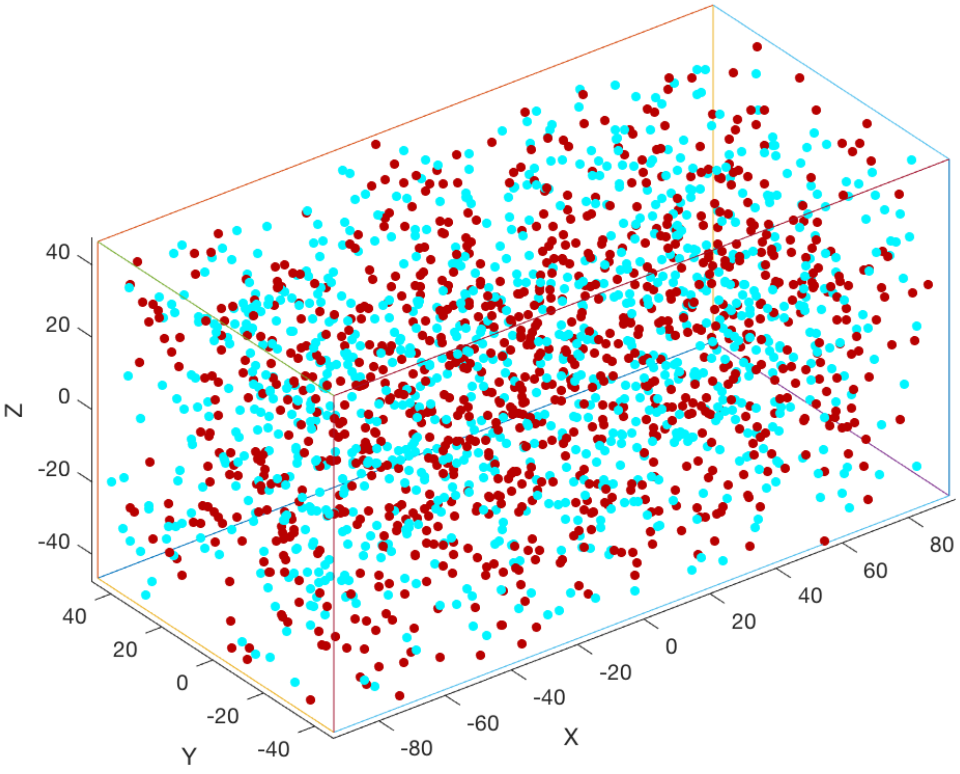

Figure 9: Particle-Tracking Based State at the End of the Second Phase

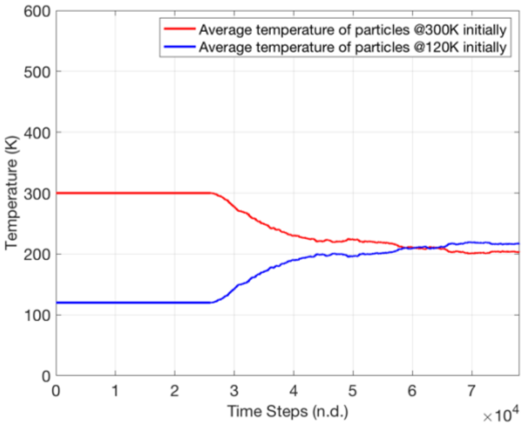

Figure 10: Particle-Tracking Based Thermal Equilibrium

Volume Based Thermal Equilibrium Analysis: Simulation results of the average temperatures inside the boundaries of the two initial systems during phases of the simulation is given in Figure 11.

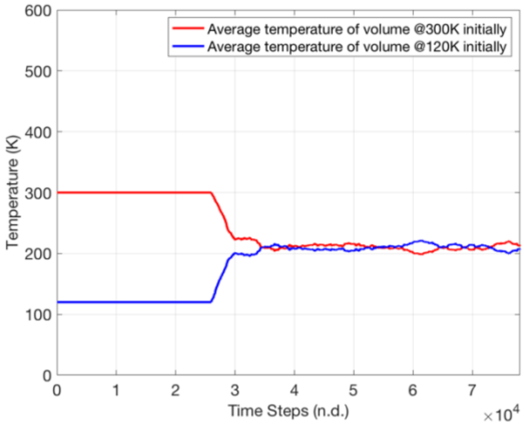

Figure 11: Volume Based Thermal Equilibrium

Thermal Diffusion

In order to calculate the thermal diffusion coefficient, the system is divided into cubical elements and average temperatures of particles in their coverage area is calculated. Then compliance of the simulation results to the Heat Equation, presented in Equation 44, is checked.

44

$$\frac{\partial T}{\partial t} = \alpha\left(\frac{\partial^2 T}{\partial x^2} + \frac{\partial^2 T}{\partial y^2} + \frac{\partial^2 T}{\partial z^2}\right)$$

In equation 45, $\boldsymbol{T}$ is the temperature of the system and $\boldsymbol{\alpha}$ is the thermal diffusivity of the medium which is further described in Equation 45:

45

$$\alpha = \frac{k}{c\rho}$$

where $\boldsymbol{k}$ is the thermal conductivity of the material, $\boldsymbol{c}$ is the specific heat capacity and $\boldsymbol{\rho}$ is the mass per unit volume. Using the available data and simulation results, the average of thermal conductivity during the second phase of the simulation is calculated as 0.0115 Watts per meter Kelvin. Since the simulation is conducted with only 2000 particles, there exist some peak and minus values. This is because the number of particles is low for making such statistical analysis. When the peak and minus values are removed, i.e. results between 0 and 0.0400 are taken into consideration, corrected thermal conductivity is found as 0.0141 Watts per meter Kelvin.

k in Literature [W/mK]			**k Results in Simulation [W/mK]**	
At 100 [K]	**At 200 [K]**	**At 300 [K]**	**Average at 210 [K]**	**Corrected Average at 210 [K]**
0.0062	0.0124	0.0179	0.0115	0.0141

Table 4: Comparison of Thermal Conductivity Results with the Literature

CONCLUSION

Establishment of the equilibrium states of the initial set up, represented in Figure 1, are analyzed. In Figure 5 and Figure 6, the distribution of the velocity along any coordinate axis is understood to be the Gaussian type for each separated system. As it can be seen in the same figures, average speeds of particles are conserved but the speed distribution is formed very similar to the Maxwell-Boltzmann distribution. Therefore, the speeds of particles are defined in an interval. Since the average speed of each system remains the same; in Figure 3, blue color tones appear in the negative side of the x-axis while red color tones are more dominant in the positive side of the x-axis. Effect of improvements on speed results is represented in Table 1. The accuracy of results is mostly below 1/10000. Simulation results for gas pressures from two different perspectives are very close to theoretical values as presented in Table 2. Similar results are obtained; depicted in Figure 7, Figure 8 and Table 3; for the mixing phase of the both systems. Thermal energy is distributed uniformly between the particles locations inside the boundary as given in Figure 10 and Figure 11. Thermal conductivity coefficient for the system, given in Table 4, is considerably close to the values available in literature.

To conclude, simulation results imply that this approach is convenient to investigate the behavior of fluid by using molecular dynamics simulation techniques. A significant improvement in accuracy is achieved for calculation of velocity contributions during interactions. This improvement will allow to extend duration and number of sample particles in simulations by means of preventing large accumulated errors. Therefore, further applications on fluid flow under the turbulent flow regimes, biomolecules or fracture mechanics can be accomplished.

References

Çıray, C. (2015). *A Formulation for the Activity of Simple Molecules Part I*, 8th Ankara International Aerospace Conference.

Eneren, Ş.P. (2016). *Validation of a Particle Simulation Approach*, Middle East Technical University, Ankara, Turkey.

Jones, J.E. (1924). On the Determination of Molecular Fields. — II. From the Equation of State of a Gas, Proceedings of The Royal Society A Mathematical Physical and Engineering Sciences, Vol. 106, p: 463-477.